
Article:
Thermou, G. orcid.org/0000-0002-9569-0176 and Hajirasouliha, I.M.A.N. (2018) Compressive behaviour of concrete columns confined with steel-reinforced grout jackets. Composites Part B: Engineering, 138. pp. 222-231. ISSN 1359-8368

https://doi.org/10.1016/j.compositesb.2017.11.041

Compressive Behaviour of Concrete Columns Confined with Steel-Reinforced Grout Jackets

Georgia E. Thermou[1, 2*] and Iman Hajirasouliha[1]

[1] Civil and Structural Engineering Department, The University of Sheffield, S1 3JD, Sheffield, UK
[2] Civil Engineering Department, Aristotle University of Thessaloniki, 54124, Thessaloniki, Greece (on leave)

Abstract: This paper investigates the compressive strength of concrete columns confined with a new jacketing system using high strength steel reinforced fabrics embedded in an inorganic matrix (SRG). A comprehensive experimental programme was conducted on 52 cylindrical columns with SRG jackets and 15 control specimens under monotonic uniaxial compression load. The test specimens were designed to investigate the influence of different design parameters including the density of the fabric (1, 1.57, 4.72 cords/cm), number of layers (1, 2), overlap length (24, 36 cm), bonding agent (4 different types of mortar) and the concrete strength (16 to 30 MPa). The test results highlight the efficiency of the proposed method, where one-layered and two-layered SRG jackets could increase the strength capacity of the unconfined specimens by up to 122% and 193%, respectively.

Keywords: Fabrics/textiles, Fibre/matrix bond, Mechanical testing, SRG Jackets

1. INTRODUCTION

Much of the existing building stock in developing countries was designed according to old standards (with little or no seismic provisions) using poor material and construction practices. Moreover, deterioration of structural elements due to ageing and aggressive environmental conditions is another factor that can significantly increase the vulnerability of reinforced

* Corresponding author, tel: +44 (0) 114 222 5710, fax: +44 (0) 114 222 5700, g.thermou@sheffield.ac.uk

concrete (RC) structures. The retrofit of deteriorated or seismically deficient structures provides a feasible and economic approach to improving their load carrying capacity and reducing their vulnerability.

In recent years, the use of composite materials in retrofitting of existing structures has been increased substantially and proved to be efficient in accommodating deterioration of structural elements or damages observed after strong earthquakes [e.g. 1, 2]. Externally Bonded Fibre Reinforced Polymers (EB-FRP) applications have gained ground due to the advantages such as high resistance to corrosion, excellent durability, high strength to weight ratio and adaptability of the technique to different types of structural members. However, there are a few shortcomings related to the high cost, toxicity, poor behaviour at high temperatures and lack of vapour permeability. The replacement of organic to inorganic matrix, cement-based mortars, seems to minimize these drawbacks. Within this context, the first applications developed with carbon sheets combined with inorganic matrix are related to flexural strengthening of beams [3-5]. This was further extended to confinement of concrete columns, where unidirectional carbon sheets with mortar matrix were utilized [6].

In the last decade, several composite systems with inorganic binders have been developed for flexural and shear strengthening and confinement of RC members using different types of fabrics and inorganic matrixes. The most popular systems are bidirectional textiles made of continuous carbon fibers embedded in cement-based mortars (Textile-Reinforced Mortar (TRM) systems) [e.g. 7-9], high strength steel and carbon fabrics combined with inorganic geopolymer resins [e.g. 10-12], PBO (poliparafenilen benzobisoxazole) nets embedded in cementitious matrix [e.g. 13, 14] and high strength steel fabrics combined with cementitious grout (SRG) [e.g. 15-25]. In general, the success in these composite systems relies on the bond characteristics between the fabric and the binding material as well as to the penetration and impregnation of the fiber sheets with inorganic binders.

Previous studies on the effect of Steel-Reinforced Grout (SRG) jackets on confined concrete have shown the efficiency of the proposed system in increasing substantially both compressive strength and deformation capacity [17-19]. These experimental studies investigated the effects of density of the fabric (for an uninhibited flow of mortar) and the overlap length on the failure modes. However, further studies are required to obtain a balance between the strength of the fabric (i.e. density) and the properties of the grout, and to investigate the effect of using multiple layers on the compressive strength and deformation capacity of the specimens and the required overlap length.

The main objective of the current study was to investigate the efficiency of SRG jackets when applied on plain concrete cylindrical columns using different design parameters. An extensive experimental study was conducted, where 52 columns confined with SRG jackets along with 15 control specimens were tested under monotonic uniaxial compression. The SRG jacketing technique proved to be very efficient in increasing both strength and deformation capacity.

2. EXPERIMENTAL PROGRAM

2.1 Specimen details - Parameters of study

Fifty-two cylindrical columns with a diameter of 150 mm and a height of 300 mm were wrapped with the SRG jacketing system and subjected to monotonically increasing concentric uniaxial compression load up to failure. The test specimens were designed to investigate the influence of the following design parameters: (i) the density of the fabric, (ii) the number of layers, (iii) the overlap length, (iv) the type of the bonding agent and (v) the concrete strength.

The specimens were cast using five concrete batches corresponding to different values of concrete compressive strength ranged between f'_{co}=16~30 MPa. The lower and upper bound

values are representative of the old and typical construction practice in the Mediterranean region and many developing countries, respectively. The variability of f'_{co} has enabled the assessment of the impact of the unconfined concrete strength on the efficiency of the SRG system. The concrete compressive strength for each batch was measured by using three 150×300mm cylindrical specimens (15 control specimens in total). The following average compressive strengths were recorded at the day of the tests: Group A: f'_{co}=23.4 MPa, Group B: f'_{co}=16.8 MPa, Group C: f'_{co}=20.7 MPa, Group D: f'_{co}=18.3 MPa and Group E: f'_{co}=30.0 MPa.

The three steel reinforced fabrics, 12X, 3X2, 3X2*, used in the experimental program comprise unidirectional steel cords fixed to a fibreglass micromesh to facilitate installation (see Fig. 1). The 12X wire cord (Fig. 1(a)) is made by twisting two different individual wire diameters together in 12 strands with over twisting of one wire around the bundle. The 3X2 and 3X2* wire cords have identical geometry and structure corresponding to five individual wires twisted together (three straight filaments wrapped by two filaments at a high twist angle, Fig. 1(b)). However, their mechanical properties are different as shown in Table 1. In the same Table, the geometrical and mechanical properties of different types of single cords used in this study are provided. The 12X and 3X2 steel fabrics (used in the specimens of Groups A and B) have a micro-fine brass coating to enhance their corrosion resistance. The 3X2* steel fabric (used in the specimens of Groups C, D, E) has been galvanized and possesses high durability in a chloride, freeze-thaw and high humidity environment.

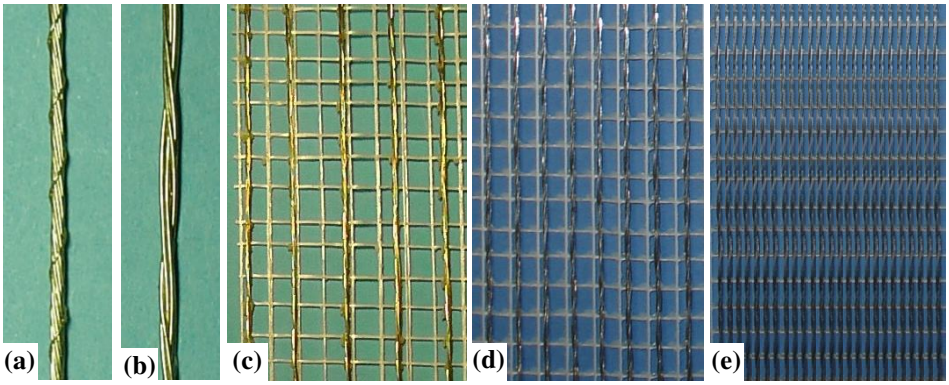

Figure 1: High strength steel cord types (a) 12X; (b) 3X2; The density of the fabrics used (c) 1.0 cord/cm; (d) 1.57 cords/cm; (e) 4.72 cords/cm.

Table 1: Geometrical and mechanical properties of single cords as provided by the manufacturers.

Fabric type	**Cord diameter (mm)**	**Cord area (mm^2)**	**Break load (N)**	**Tensile strength, $f_{fu,s}$ (MPa)**	**Strain to failure, $\varepsilon_{fu,s}$ (mm/mm)**	**Elastic modulus, E_f (MPa)**	**Axial stiffness, K_f (MPa) - single layer**
12X	0.889	0.621	1250	2014	0.019	110000	6820 (1 cord/cm)
3X2	0.889	0.621	1539	2480	0.021	120000	7440 (1 cord/cm)
3X2*	0.827	0.538	1506	2800	0.015	190000	15960 (1.57 cords/cm) 48260 (4.72 cords/cm)

The spacing between successive cords, which defines the density of the steel fabric, is one of the key design parameters of the SRG jacketing technique as has been highlighted by Thermou et al. [16-20]. While the spacing should be wide enough as to provide uninhibited flow of the cementitious grout through the steel fabric, it should be designed to develop adequate bond between the fabric and the matrix. In this study, three different densities 1, 1.57 and 4.72 cords/cm are examined as shown in Figures 1(c) to (e). The equivalent thickness per unit width for a single layer of steel fabric, t_s, was calculated to be 0.062, 0.084 and 0.254 mm for the 1, 1.57 and 4.72 cords/cm, respectively. The axial stiffness of the steel fabric, K_f ($=t_s \cdot E_f$), which also appears in Table 1, is directly related to the density of the fabric (the numbers in Table 1 should be doubled for the two-layered jackets).

In general, the overlap length should be sufficient to avoid a premature debonding failure mode. Previous experimental studies [18, 19] indicated that the overlap length of 36 cm usually provides adequate anchorage for the single layered SRG jacketed cylindrical specimens to allow the tensile fracture of the fabric. To investigate this further, in the current

study two different overlap lengths of 24 and 36 cm were used for the specimens with two- and the one-layered jackets, respectively.

Four different types of mortars were selected to provide different mechanical properties as presented in Table 2. The objective was to assess on one hand the impact of the mortar flexural strength on the compressive strength of SRG confined concrete and on the other hand the role of the adhesive bond strength on the composite behaviour of the SRG system. For the specimens of Groups A and B, a commercial fiber reinforced cementitious grout with pozzolanic additives, classified as M1 and two custom-made inorganic mortars M2 and M3 were used. M2 comprises of NC182 cement enriched with nanoparticles N20 (nanosilica, surface area: BET m2/g 200±25), whereas M3 uses NC182 cement with propylene fibers and additional anticorrosive. In Groups C, D and E, a commercial geo-mortar M4 is used which has a crystalline reaction geobinder base with very low petrochemical polymer content and free from organic fibers. The adhesive bond of the mortars M2 and M3 was measured according to standard BS EN 12636:1999 [26].

Table 2: Mechanical properties of the utilized mortars at 28 days.

Mortar	Modulus of elasticity, E_m (MPa)	Flexural strength, f_{mf} (MPa)	Compressive strength, f_{mc} (MPa)	Adhesive bond strength, f_{mb} (MPa)
M1	8030	6.78	22.10	1.88
M2	10352	1.00	4.06	2.94
M3	18629	4.24	20.10	4.31
M4	25000	10.00	55.00	2.00

The test specimens were given the notation Gi#L_N, where G stands for the group of the specimens (A, B, C, D, E in Table 3), i (=1 to 10) corresponds to the type of the SRG jacketing system, L indicates the number of fabric layers (1 and 2) and N refers to the specimen number for each subgroup of the identical specimens. The type of the SRG jacketing system is related to the type of fabric (12X, 3X2 and 3X2*), the density of the fabric (1, 1.57 and 4.72 cords/cm), the overlap length (24 cm and 36 cm) and the type of inorganic matrix (M1, M2, M3, M4) as defined in Table 3. For example, A2#1_1 specimen belongs to

the Group A and refers to the first specimen of the subgroup constructed with the one layer Type 2 SRG jacket which is made by using mortar M1, 3X2 steel reinforced fabric of 1 cord/cm density and overlap length of 36 cm. The details of all test specimens are given in Table 3.

It should be noted that the specimens with 12X fabric were mainly used as a pilot study and, therefore, their repeatability was not assessed. However, the results of these specimens can provide good insight to the effectiveness of SRG jacketing system using different types of steel fabrics as will be discussed in the next sections.

Table 3: Specimen details.

Group	Notation	f'_{co} (MPa)	Type of jacket	Type of fabric	Density (cords/cm)	Number of layers	Overlap length (cm)	Type of Mortar	Number of specimens
Group A	A	23.14	-	control	-	-	-	-	3
	A1#1		1	12X	1	1	36	M1	1
	A2#1		2	3X2	1	1	36	M1	2
	A2#2		2	3X2	1	2	36	M1	3
	A3#1		3	12X	1	1	36	M2	1
	A4#1		4	3X2	1	1	36	M2	2
	A4#2		4	3X2	1	2	36	M2	3
	A5#1		5	12X	1	1	36	M3	1
	A6#1		6	3X2	1	1	36	M3	2
	A6#2		6	3X2	1	2	36	M3	3
Group B	B	16.62	-	control	-	-	-	-	3
	B1#1		1	12X	1	1	36	M1	1
	B3#1		2	12X	1	1	36	M2	1
	B5#1		3	12X	1	1	36	M3	1
Group C	C	20.73	-	control	-	-	-	-	3
	C7#1		7	3X2*	1.57	1	24	M4	3
	C8#1		8	3X2*	1.57	1	36	M4	2
	C7#2		7	3X2*	1.57	2	24	M4	2
	C8#2		8	3X2*	1.57	2	36	M4	2
Group D	D	18.27	-	control	-	-	-	-	3
	D8#1		8	3X2*	1.57	1	36	M4	3
	D7#2		7	3X2*	1.57	2	24	M4	3
	D9#1		9	3X2*	4.72	1	36	M4	3
	D10#2		10	3X2*	4.72	2	24	M4	2
Group E	E	29.98	-	control	-	-	-	-	3
	E8#1		8	3X2*	1.57	1	36	M4	2
	E7#2		7	3X2*	1.57	2	24	M4	3
	E9#1		9	3X2*	4.72	1	36	M4	3
	E10#2		10	3X2*	4.72	2	24	M4	3
								Total	67

2.2 SRG jacketing method

The SRG jacketing procedure started with the preparation of the steel reinforced fabrics. The sheets were cut into the desired lengths taking into account the number of layers and the

overlap length and then bent in order to facilitate the wrapping process (Fig. 2a). After removing the metallic moulds, the substrate of the unconfined cylindrical specimens was cleaned and saturated with water before putting a layer of the cementitious grout (Fig. 2b). In case of specimens of Group C, the surface was roughened manually with chisel and hammer to enhance the bond between the substrate and the mortar (Fig. 2c). The cementitious grout was applied manually with the help of a trowel directly onto the lateral surface of the specimens (Fig. 2d). The steel fabric was placed immediately after the application of the cementitious grout (Fig. 2e). The grout was then squeezed out between the steel fibers by applying pressure manually. After having placed one or two layers of fabric, the remaining length was lapped over the lateral surface. It should be mentioned that using the dense fabric (4.72 cords/cm) imposed some difficulties in the penetration of the mortar through the small gaps. Additionally, handling of the dense fabric, although it was pre-bent, was difficult due to its high axial stiffness.

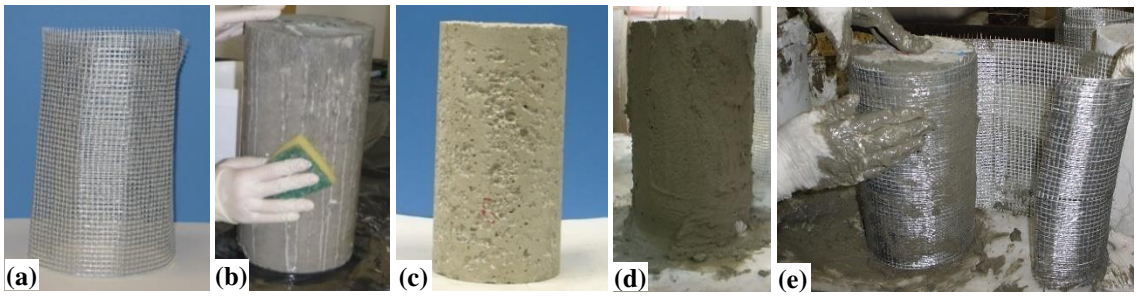

Figure 2: SRG jacketing method: (a) Preparation of the fabric; (b) Saturation of the specimen with water; (c) Roughening of the interface (only in Group C); (d) Application of a thin layer of cementitious grout; (e) Application of the steel-reinforced fabric.

A final layer of the cementitious grout was applied to the exposed surface. The thickness of the grout layer including the steel reinforced fabric was 7 and 10 mm for one- and two-layered jackets, respectively, allowing the steel fabric to be fully embedded in the cementitious matrix. The SRG jackets were fabricated to be 28 cm in height leaving 1 cm gap between the steel bearing plates of the loading machine and the steel fabric to prevent any direct axial load on the jacket.

2.3 Instrumentation and testing procedure

Fig. 3 shows the experimental test-set up used in this study. The monotonic loading was applied at a rate of 0.15 MPa/s in load control, using a 6000 kN compression testing machine. The post-peak branch of the axial stress-strain curve was obtained through a controlled release of the hydraulic oil pressure of the testing machine to have similar displacement rate as that in the ascending part of the loading. The same approach has been followed by many researchers in the past (e.g. [27]). Axial strain was calculated from the average measurements of four linear variable differential transducers (LVDTs) mounted on the upper and lower steel frames fixed to the specimen divided by the gauge length which was equal to 150 mm (Fig. 3). Axial load was measured by a load cell placed at the top of the specimens. Due to experimental constrains, it was not possible to provide accurate and reliable measurements of the lateral strains in the current experimental program.

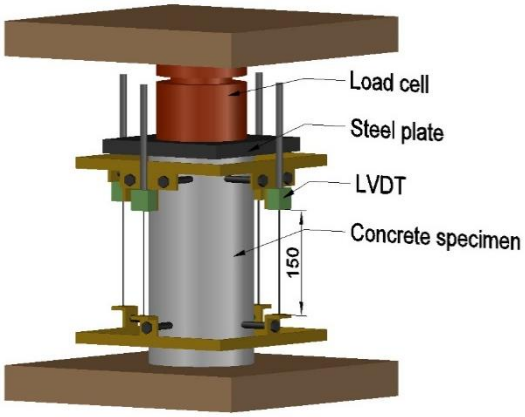

Figure 3: Test setup.

3. DISCUSSION OF THE TEST RESULTS

3.1 Parametric study

In Group A, the main objective was to study how the mechanical characteristics of the binding material and the number of layers affect the performance of SRG confined concrete for the specimens with unconfined concrete compressive strength, f'_{co}=23.4 MPa. Three types of mortar (M1, M2, M3 in Table 3) and one- and two-layers of SRG jackets were used in this

group. The Group B specimens were designed to assess the effects of using different mortars (M1, M2, M3 in Table) in the case of lower concrete compressive strength (f'_{co}=16.8 MPa). In Group C, the effects of overlap length (24 and 36 cm) along with the number of layers (one and two) were investigated for the specimens with 1.57 cords/cm fabric and f'_{co}=20.7 MPa. In Groups D and E, parameters of investigation were the density of the fabric (1.57 and 4.72 cords/cm), the number of layers (one and two), and the unconfined concrete compressive strength (f'_{co}=18 and 30 MPa).

3.2 Failure modes

The test specimens failed in three distinct modes of failure: (a) rupture of the steel fabrics, (b) debonding, and (c) mixed mode of failure where debonding was followed by rupture of the steel fabric in a limited height of the specimen (see Figs. 4 to 6).

Failure mode (a): In case of the one-layered jackets with 1 and 1.57 cords/cm and 36 cm overlap length, the rupture of the fabric was the most observed failure mode (Fig. 4). The only exceptions were two of the D8#1 sub-group specimens that failed in a mixed mode, mainly due to the fact that some of the steel cords were not well-embedded in the mortar matrix. All SRG jacketed specimens with two layers of 1 and 1.57 cords/cm fabrics (with overlap length of 24 and 36 cm) failed due to tensile fracture of the steel cords as well. This indicates that the gap between successive steel cords was adequate to allow the mortar penetrate through the fabric and develop of an interlocking mechanism between the steel cords and the inorganic matrix. Unlike the FRP confinement, the failure of SRG jackets was ductile due to the progressive fracture of the steel cords as it is also evident from the stress-strain curves shown in Fig.7.

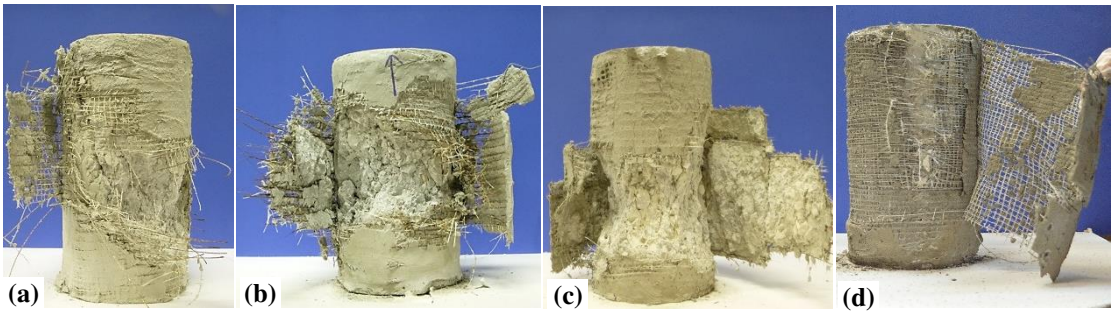

Figure 4: SRG jacketed specimens at failure due to tensile fracture of the steel cords of the fabric.

Failure mode (b): In the specimens with 1 layer of 1.57 cords/cm and 24 cm overlap length (C7#1), the debonding failure mode was observed mainly due to insufficient overlap length (Fig. 5 (a)). The specimens with 1 layer of 4.72 cords/cm (dense fabric) and 36 cm overlap length also failed due to debonding (Figs. 5 (b) and (c)).

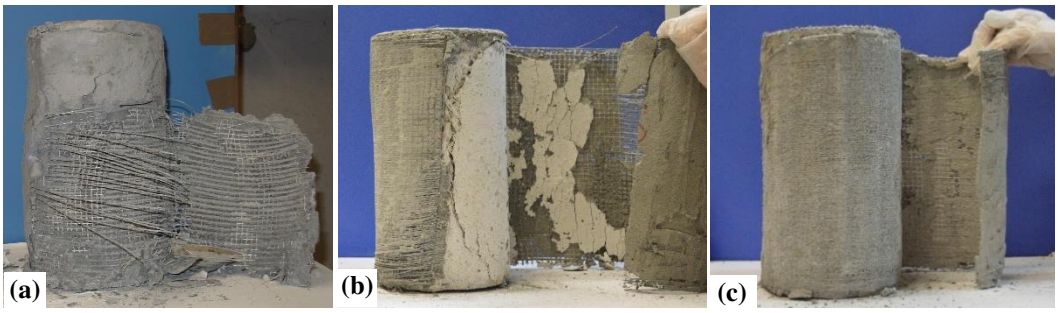

Figure 5: SRG jacketed specimens at failure due to debonding (a) one layer of 1.57 cords/cm density; (b), (c) one layer of 4.72 cords/cm density steel fabric.

Failure mode (c): As shown in Fig 6, the columns wrapped with two layers of the 4.72 cords/cm fabric exhibited a mixed mode of failure, where the external and internal layer of the jacket failed due to debonding and rupture of the steel fabric (along almost 1/3 of the specimen height), respectively. This failure mode can be attributed to the fact that, due to the high axial stiffness of the dense fabric (4.72 cords/cm), high tensile stresses were developed in the steel fabric, which could not be balanced by the shear strength of the mortar. However, the internal layer failed in rupture since the anchorage length was long enough (almost equal to the perimeter of the column) to prevent debonding. At the end of these tests, the steel cords were well embedded in the mortar along the debonding length (L_b=24 cm), which indicates

that despite some difficulties in the application of the dense fabrics (see section 2.2), the mortar penetrated successfully through the steel fabric.

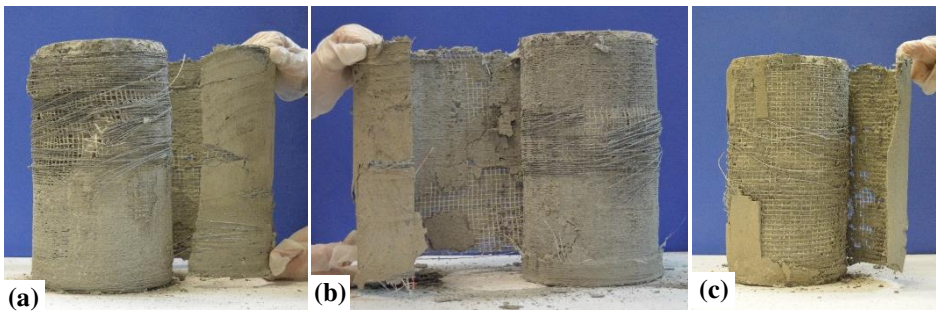

Figure 6: SRG jacketed specimens with a mixed mode of failure (a), (b) two layers; and (c) one layer of 4.72 cords/cm steel fabric.

3.3 Enhancement in strength and ultimate strain

The average stress-strain curves for the five selected groups of columns (see Table 3) are depicted in Fig. 7. In general, the results show that SRG jacketing improved substantially both the strength and the deformation capacity of the specimens. For better comparison, the results for all tested specimen are summarised in Table 4. The information provided includes the compressive strength of the unconfined concrete (f'_{co}), the confined concrete compressive strength (f'_{cc}) and the corresponding strain (ε_{cc}), the ultimate compressive strength corresponding to 20% drop in the compressive strength of confined concrete ($f'_{ccu,80\%}$ =0.80· f'_{cc}) and the corresponding strain ($\varepsilon_{ccu,80\%}$), and the strain ductility (μ_ε). The gain in the compressive strength and the ultimate strain are defined as (f'_{cc} - f'_{co})/ f'_{co} and ($\varepsilon_{ccu,80\%}$-ε_{co})/ε_{co}, respectively, where ε_{co} is considered to be 2‰. In the following, the results are discussed in details for each group of SRG confined columns.

Group A: Specimens with mortar M1, one layer of 3X2 steel fabric managed to increase the compressive strength by 40%, while two layers of fabric increased the compressive strength by 67% (see Fig. 7(a), Table 4). Similar results were obtained for the specimens with mortar M3 (39% and 64% for one and two layers, respectively) as shown in Fig. 7(c). However, Fig.

7(b) shows that the strength increase was slightly less in the specimens with mortar M2 (30% and 47% for one and two layers, respectively). This small difference is believed to be attributed to the lower flexural strength of mortar M2 compared to that of mortars M1 and M3. The interfacial shear stresses developed between the fabric and the substrate at the overlap length seem not to have exceeded the bond stress of the mortar since the failure mode was always due to the rupture of the steel fabric. This implies that even for the low adhesive bond strength (1.88 MPa as shown in Table 2), the debonding failure mode can be prevented using an overlap length of 36 cm. It is shown in Table 4 that, on average, using one layer and two layers of steel fabric could increase the ultimate strain capacity of the specimens by almost 250% and 350%, respectively.

Group B: As discussed before, all specimens in this group failed due to rupture of the fabric. Despite the small number of specimens in this group, the results are in good agreement with Group A. Therefore, it can be concluded that the type of mortar does not considerably influence the strength and deformation capacity of the SRG confined specimens when the failure mode is due to the rupture of steel fabric.

Group C: One-layered jackets with 24 cm overlap length failed due to debonding despite roughening of the concrete interface (Fig. 2(c)), whereas 36 cm overlap length provided adequate anchorage to reach the tensile fracture of the fabric. This shows that the 36 cm overlap length suggested by Thermou et al. [18] for one layer of less dense fabric (1 cord/cm density) is also adequate for the 1.57 cords/cm density fabric. The two-layered jackets with both 24 and 36 cm overlap length failed due to rupture, which implies that they require a lower overlap length to prevent debonding failure. It is shown in Fig. 7(e) and Table 4 that the strength and strain increase in the case of one-layered SRG jacket was 64% and 428%, respectively. Two-layered SRG jackets with 24 cm overlap length managed to increase the strength and strain capacity by 94% and 555%, respectively, whereas in case of 36 cm overlap length the strength and strain capacity increased by 115% and 650%, respectively.

Table 4: Experimental test results.

No	Specimen	Compr. strength, f'_{co} (MPa)	Compr. strength, f'_{cc} (MPa)		Ult. compr. strength, $f'_{ccu,80\%}$ (MPa)		Strain, ε_{cc}		Ultimate strain, $\varepsilon_{ccu,80\%}$		f'_{cc} / f'_{co}	$\varepsilon_{ccu,80\%}$/ $\varepsilon_{co}^{\#}$	Strain ductility, μ_{ε}		Failure mode
		value	**value**	**mean**	**value**	**mean**	**value**	**mean**	**value**	**mean**			**value**	**mean**	
1	A1#1	23.14	28.75	28.75	23.00	23.00	0.0035	0.0035	0.0069	0.0069	1.24	3.45	2.47	2.5	R
2	A2#1-1	23.14	31.79	32.30	54.43	40.34	0.0038	0.0035	0.0076	0.0071	1.40	3.55	2.41	2.3	R
3	A2#1-2		32.81		26.25		0.0032		0.0066				2.27		R
4	A2#2-1	23.14	35.96	38.56	28.77	31.80	0.0080	0.0095	0.0095	0.0103	1.67	5.17	3.25	3.2	R
5	A2#2-2		40.61		32.49		0.0102		0.0106				3.16		R
6	A2#2-3		39.11		34.13		0.0104		0.0109				3.20		R
7	A3#1	23.14	29.80	29.80	23.84	23.84	0.0043	0.0043	0.0058	0.0058	1.29	2.90	1.98	2.0	R
8	A4#1-1	23.14	31.72	30.12	25.38	24.10	0.0034	0.0040	0.0052	0.0073	1.30	3.18	1.60	3.1	R
9	A4#1-2		28.51		22.81		0.0045		0.0093				4.61		R
10	A4#2-1	23.14	35.73	34.02	28.58	27.22	0.0068	0.0072	0.0072	0.0079	1.47	3.97	2.19	2.1	R
11	A4#2-2		31.56		25.25		0.0082		0.0087				1.66		R
12	A4#2-3		34.77		27.82		0.0067		0.0079				2.50		R
13	A5#1	23.14	33.07	33.07	26.46	26.46	0.0047	0.0047	0.0059	0.0059	1.43	2.95	2.01	2.0	R
14	A6#1-1	23.14	30.00	32.15	24.01	25.73	0.0046	0.0045	0.0082	0.0076	1.39	3.78	2.81	2.3	R
15	A6#1-2		34.30		27.44		0.0044		0.0069				1.86		R
16	A6#2-1	23.14	37.51	38.02	30.01	30.42	0.008	0.0080	0.0088	0.0086	1.64	4.30	2.13	1.9	R
17	A6#2-2		40.39		32.31		0.0085		0.0089				1.82		R
18	A6#2-3		36.17		28.94		0.0074		0.0081				1.78		R
19	B1#1	16.62	30.45	30.45	24.37	24.37	0.0042	0.0042	0.0069	0.0069	1.83	3.45	2.28	2.3	R
20	B2#1		26.64	26.64	21.31	21.31	0.0049	0.0049	0.0055	0.0055	1.60	2.75	2.31	2.3	R
21	B3#2		28.32	28.32	22.66	22.66	0.0056	0.0056	0.0077	0.0077	1.70	3.85	2.43	2.4	R
22	C7#1-1*	20.73	30.71	31.36	24.22	24.64	0.0066	0.0071	0.0092	0.0121	1.51	3.45	-	-	D
23	C7#1-2*		31.83		23.49		0.0097		0.0121				-		D
24	C7#1-3*		31.55		26.22		0.0051		0.0151				-		D
25	C8#1-1	20.73	33.82	34.10	26.77	26.58	0.011	0.0095	0.0111	0.0106	1.64	5.28	6.71	7.7	R
26	C8#1-2		34.38		26.38		0.0079		0.0100				8.61		R

A common value for ε_{co} equal to 2 ‰ is considered in order for the $\varepsilon_{ccu,80\%}$ values of columns to be compared. The symbol (*) identifies the columns that failed due to debonding. R: rupture failure mode, D: debonding failure mode, M: mixed mode of failure

Table 4-cont.: Experimental test results.

No	Specimen	Compr. strength, f'_{co} (MPa)	Compr. strength, f'_{cc} (MPa)		Ult. compr. strength, $f'_{ccu,80\%}$ (MPa)		Strain, ε_{cc}		Ultimate strain, $\varepsilon_{ccu,80\%}$		f'_{cc} / f'_{co}	$\varepsilon_{ccu,80\%}$/ ε_{co}#	Strain ductility, μ_ε		Failure mode
		value	**value**	**mean**	**value**	**mean**	**value**	**mean**	**value**	**mean**			**value**	**mean**	
27	C7#2-1	20.73	41.05	40.24	32.88	31.02	0.0088	0.0104	0.0125	0.0131	1.94	6.55	9.40	9.7	R
28	C7#2-2		39.43		29.16		0.012		0.0137				10.00		R
29	C8#2-1	20.73	42.66	44.63	33.99	35.69	0.0143	0.0124	0.0163	0.0150	2.15	7.50	10.35	10.1	R
30	C8#2-2		46.60		37.38		0.0104		0.0137				9.80		R
31	D8#1-1	18.27	27.53	27.68	22.02	22.14	0.0102	0.0099	0.0112	0.0136	1.51	6.82	12.95	14.0	R
32	D8#1-2		27.08		21.66		0.0035		0.0129				13.95		M
33	D8#1-3		28.42		22.73		0.016		0.0168				15.12		M
34	D7#2-1	18.27	34.99	36.44	27.99	29.15	0.009	0.0102	0.0149	0.0130	1.99	6.48	13.47	11.9	R
35	D7#2-2		36.33		29.06		0.011		0.013				11.90		R
36	D7#2-3		38.00		30.40		0.0105		0.011				10.42		R
37	D9#1-1*	18.27	46.47	40.64	37.18	35.21	0.015	0.0090	0.0154	0.0098	2.22	4.92	-	-	D
38	D9#1-2*		40.56		40.56		0.006		0.006				-		D
39	D9#1-3*		34.88		27.90		0.006		0.00809				-		D
40	D10#2-1	18.27	47.00	53.53	47.00	47.53	0.0120	0.01750	0.0120	0.0180	2.93	9.00	2.80	8.6	M
41	D10#2-2		60.06		48.05		0.0230		0.0240				14.3		M
42	E8#1-1	29.98	40.90	40.51	32.72	32.41	0.0045	0.0035	0.0133	0.0133	1.35	6.65	16.74	16.7	R
43	E8#1-2		40.12		32.09		0.0024		-				-		R
44	E7#2-1	29.98	44.58	45.21	35.66	36.17	0.004	0.0077	0.0112	0.0123	1.51	6.15	6.82	6.3	R
45	E7#2-2		46.25		37.00		0.008		0.0133				6.50		R
46	E7#2-3		44.80		35.84		0.011		0.0124				5.44		R
47	E9#1-1*	29.98	49.03	45.87	39.23	36.70	0.0045	0.0047	0.0045	0.0065	1.53	3.23	-	-	D
48	E9#1-2*		46.02		36.82		0.003		0.0084				-		D
49	E9#1-3*		42.57		34.06		0.0065		0.0065				-		D
50	E10#2-1	29.98	68.42	64.19	54.74	51.35	0.0112	0.0091	0.01417	0.0105	2.14	5.27	7.64	5.0	M
51	E10#2-2		64.52		51.62		0.009		0.01033				5.32		M
52	E10#2-3		59.62		47.70		0.007		0.0071				2.05		M

A common value for ε_{co} equal to 2 ‰ is considered in order for the $\varepsilon_{ccu,80\%}$ values of columns to be compared. The symbol (*) identifies the columns that failed due to debonding. R: rupture failure mode, D: debonding failure mode, M: mixed mode of failure

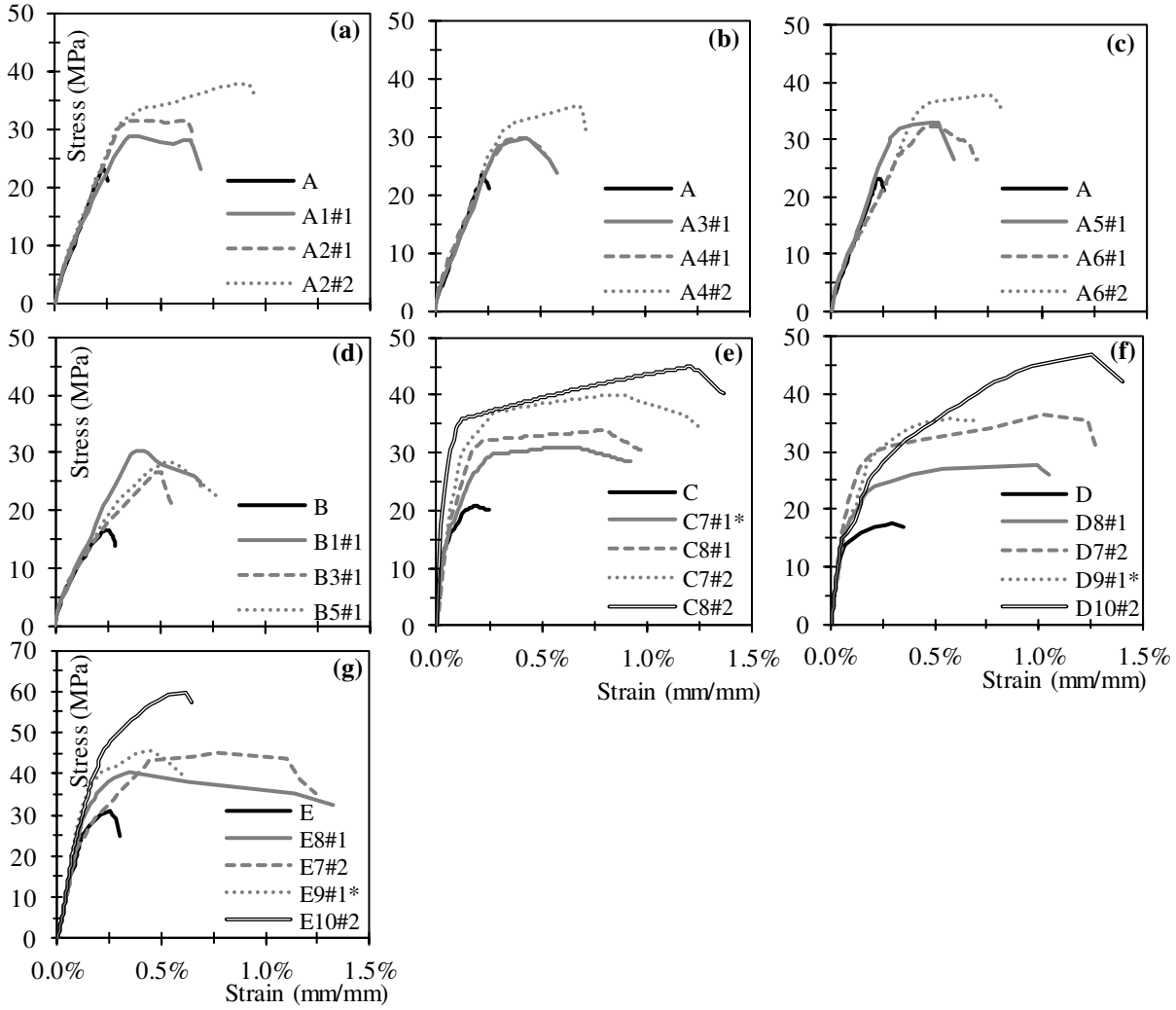

Groups D and E: In general, a good agreement was observed in the failure mode of the one- and two-layered SRG jackets between Groups D and E as discussed in the previous section. It is shown in Table 4 that the ultimate strain increase ranged between 548% and 755% in Group D and between 427% and 565% in Group E. The strength increase for the same sub-group of specimens ranged between 51% and 193% in Group D and between 35% and 114% in Group E. The above results show that the effectiveness of SRG jackets increases as the unconfined concrete strength decreases, which is in line with the observations made by [e.g. 7, 18, 19].

Figure 7: Comparison of the average stress – strain curves for the SRG-jacketed specimens of: (a), (b), (c) Group A using different mortars, (d) Group B, (e) Group C, (f) Group D and (g) Group E.

3.4 Effects of key design parameters

In this section, the effects of key design parameters including the density of the steel fabrics, number of layers and concrete compressive strength on the performance of SRG jacketing system is investigated. For better comparisons, the average increase in the strength and deformation capacity of the specimens were estimated for the subgroups with the same concrete compressive strength, density and number of layers as shown in Table 5. The effectiveness of various SRG jacketing arrangements with different fabric densities and number of layers can be assessed by considering their axial stiffness, k_f (see Table 1).

Table 5: Average strength and strain increase of the specimens tested.

Group	Compr. strength, f'_{co} (MPa)	Fabric type	Density (cords/cm)	Layers	Strength increase (%)	Strain increase (%)	Mode of failure
A	23.14	12X	1	1	32	210	R
		3X2	1	1	36	250	R
		3X2	1	2	59	348	R
B	16.62	12X	1	1	71	235	R
C	20.73	3X2*	1.57	1	64	428	R
		3X2*	1.57	2	105	603	R
D	18.27	3X2*	1.57	1	51	582	R/M
		3X2*	1.57	2	99	548	R
		3X2*	4.72	2	193	755	M
E	29.98	3X2*	1.57	1	35	565	R
		3X2*	1.57	2	51	515	R
		3X2*	4.72	2	114	427	M

Comparisons are made only between sub-group of specimens that failed due to rupture of the fabric and mixed mode of failure. As discussed before, the type of mortar did not seem to influence considerably the strength and deformation capacity of the specimens when the failure mode was due to the rupture of steel fabric. Therefore, the effect of using mortars with different characteristics was not considered in this section. Previous research has shown that the axial stiffness of steel fabrics plays an important role in the compressive strength and strain capacity of SRG jacketed specimens [18, 19]. Therefore, for a better comparison, the results are also discussed based on the axial stiffness ratio, k_f, which is defined as the ratio of

the axial stiffness of the stronger to the weaker SRG system. The specimens tested in this study were designed to cover the axial stiffness ratios of $\mathbf{k_f}$=2, 3 and 6.

Axial stiffness ratio k_f=2: The response of one- and two-layered SRG jackets with the same fabric density are compared. In Group A (1 cord/cm 3X2 fabric and f'_{co}=23.1 MPa), the two-layered SRG jackets on average increased the strength and ultimate strain capacity of the specimens by 64% and 39%, respectively. Almost the same level of strength and strain increase (64% and 41%) was observed in Group C, which has a lower average concrete strength (f'_{co}=20.7 MPa) and stiffer fabric (1.57 cords/cm 3X2*). Adding a second layer of steel fabric to the specimens in Group D (1.57 cords/cm 3X2* fabric and f'_{co}=18MPa), increased the axial strength by 94%. However, for the same SRG jacket configuration but with the concrete compressive strength of f'_{co}=30 MPa (Group E), the second layer of steel fabric could increase the axial strength only by 46%. Adding the second layer of SRG jacket in Groups D and E did not considerably change the ultimate strain capacity of the specimens. Overall, these results suggest that, for the same axial stiffness ratio, the second layer of steel fabric can be considerably more efficient for the specimens with lower unconfined concrete compressive strength. This is in agreement with the observation made in section 3.2 that the effectiveness of SRG jackets in general increases as the unconfined concrete strength decreases.

Axial stiffness ratio k_f=3: This value corresponds to the two-layered SRG jackets made by 4.72 and 1.57 cords/cm fabrics. It is shown that using the denser fabric in this case could increase the strength capacity of the two-layered specimens by 95% and 124% for the specimens of Group D and E, respectively. However, the denser fabric did not always improve the strain capacity of the confined specimens. While the strain capacity increased by 38% for Group D, a reduction of 17% was observed for the specimens of Group E.

Axial stiffness ratio k_f=6: The specimens with two-layered 4.72 cord/cm jackets are compared with those with one-layered of 1.57 cords/cm jacket. The strength capacity increase for this axial stiffness ratio was 275% and 226% for the specimens of Group D and Group E, respectively. Following a similar trend as the previous case, the strain capacity increased by 30% for the specimens of Group D, whereas a reduction of 24% was observed for the specimens of Group E.

The results discussed above indicate that using higher density fabrics (two layered of 4.72 cords/cm fabrics) can considerably increase the axial strength of the SRG jacketed systems, while it may reduce the strain capacity of the specimens with higher compressive strength. This can be attributed to the fact that these specimens exhibited a mixed mode of failure (as discussed in previous sections), and therefore, the maximum strain capacity was not reached.

4. ANALYTICAL INVESTIGATION

4.1 Interpretation of the modes of failure

The critical mode of failure in SRG jacketing system is directly linked to the mechanical characteristics of the fabric and the mortar as well as to the bond mechanism between the concrete and the mortar, and the mortar and the steel cords. The limiting transverse effective stress, $f_{s,eff}$, in the steel reinforced fabric can be defined by the minimum of the transverse stress corresponding to the rupture of the steel reinforced fabric, $f_{s,rupt}$, and the debonding stress between the jacket and the mortar, $f_{s,deb}$, along the overlap length, L_b. The effects of using different overlap lengths in providing adequate anchorage of the high strength steel fabric have been investigated in the previous studies on concrete confinement of cylindrical columns [17, 18].

The debonding stress $f_{s,deb}$ is influenced by both the characteristics of the mortar (interfacial bond stress) and the thickness of the fabric. The mortar is considered as the weak

link of the composite system developing a brittle mode of failure when the ultimate shear strength (bond stress), $f_{mb,}$ is reached [18]. Therefore, the proposed composite system is considered successful when rupture of the fabric occurs before mortar reaches its ultimate shear strength. This type of failure was observed in the majority of the current experimental programme (83% of the SRG jacketed specimens failed due to fabric rupture). Considering the force equilibrium along the overlap length, L_b, rupture of the fabric is expected when:

$$\varepsilon_{s,rupt} < \frac{L_b \cdot f_{mb}}{t_s \cdot E_f} \tag{1}$$

where t_s is the equivalent thickness of the fabric, E_f is the modulus of elasticity and f_{mb} is the ultimate shear stress of the mortar. $\varepsilon_{s,rupt}$ is the strain at which rupture of the fabric occurs given as a fraction of the ultimate strain capacity of the steel fabric, $\varepsilon_{fu,s}$ (see Table 1). The strain efficiency factor, $k_\varepsilon(=\varepsilon_{s,rupt}/\varepsilon_{fu,s})$, adopted herein is 0.55 which corresponds to the average k_ε value evaluated experimentally for the Steel-Reinforced Polymer (SRP) jacketed cylinders (i.e. steel fabrics combined with organic matrix (resin)) [28, 29]. It is noted that further studies are needed for determining the strain efficiency factor in case of square/rectangular cross sections as suggested by Nisticò and Monti [30] and Nisticò [31]. Subsequently, the lateral confining pressure provided by the steel fabric with the cords circumferentially aligned and covering the total concrete surface can be calculated by the following equation originally developed for FRP confinement [32] (see Fig. 8):

$$\sigma_{lat} = \frac{1}{2} K_{eff} \cdot \rho_{SRG} \cdot E_f \cdot \varepsilon_{s,rupt} \tag{2}$$

where ρ_{SRG} $(=4 \cdot t_s/D)$ is the volumetric ratio of the SRG jacket, E_f is the modulus of elasticity, $\varepsilon_{s,rupt}$ is the rupture strain of the fabric. K_{eff} is the effectiveness coefficient taken equal to one for all fabrics examined herein considering that the effectiveness of confinement along the height of the specimen is not influenced by the finite gaps between cords [18]. Hence, the

steel fabric was considered as a continuous fabric along the height of the specimen with an equivalent thickness t_s. The lateral confining pressure can be further simplified to:

$$\sigma_{lat} = \frac{2}{D} \cdot t_s \cdot E_f \cdot \varepsilon_{s,rupt} \tag{3}$$

where D(=150 mm) is the diameter of the cylindrical column. The term ($t_s \cdot E_f$) in Eqs. (1) and (3) corresponds to the axial stiffness of the steel fabric, K_f, which also controls the mode of failure. For comparison purposes, the axial stiffness of a commonly used carbon fabric in practice is estimated equal to 25300 N/mm (=0.11×230000, where 0.11 mm is the thickness of the fabric and 230000 MPa is the modulus of elasticity). This implies that two layers of 1.57 cord/cm can provide comparable axial stiffness values to CFRP jackets.

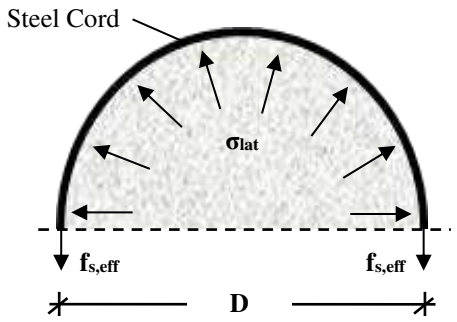

Figure 8: Lateral confining pressure, σ_{lat}, exerted by the steel cord.

The anticipated mode of failure was evaluated for all tested specimens based on Eq. (1). In general, the predicted failure modes were in very good agreement with the experimental observations. Based on the analytical calculations, the debonding failure mode is expected in the case of one- and two-layered jackets when the 4.72 cords/cm 3X2* fabric is used. For the case of two-layered 1.57 cords/cm 3X2* fabric with 24 cm overlap length, the $\varepsilon_{s,rupt}$ was equal to ($L_b \cdot f_{mb}/t_s \cdot E_f$), and therefore, both modes of failure could be practically observed. The dominant failure mode for the rest of the specimens was predicted to be due to the rupture of the steel fabrics.

4.2 Confinement effectiveness

The confinement effectiveness of columns jacketed with composite fabrics (e.g. FRPs) can be assessed by estimating the Modified Confinement Ratio (MCR) as suggested by Mirmiran

et al. [33]. In case of cylindrical columns, the confinement ratio is defined as the ratio σ_{lat}/f'_{co}, where σ_{lat} is the lateral confining pressure exerted by composite jackets and f'_{co} is the compressive strength of unconfined concrete. In the study of Spoelstra and Monti [34] a minimum value of σ_{lat}/f'_{co} =0.07 was suggested for sufficient confinement in case of FRP wrapping. This limit value was also adopted by Teng et al. [35].

Fig 9(a) shows the normalized compressive strength, f'_{cc}/f'_{co}, versus the MCR of the specimens that failed due to rupture of the steel fabric and the mixed mode of failure. It is observed that for the 1 cord/cm fabric with f'_{co} ranging between 16 to 23 MPa (Groups A and B), the MCR was between 0.04 to 0.10. For the 1.57 and 4.72 cords/cm fabrics with f'_{co} =18~30 MPa (Groups C to E), the MCR was 0.06 to 0.19 and 0.35 to 0.58, respectively. This implies that in case of SRG jackets sufficient confinement could be provided even for confinement ratio values lower than 0.07 which is the limit identified for FRP confined concrete.

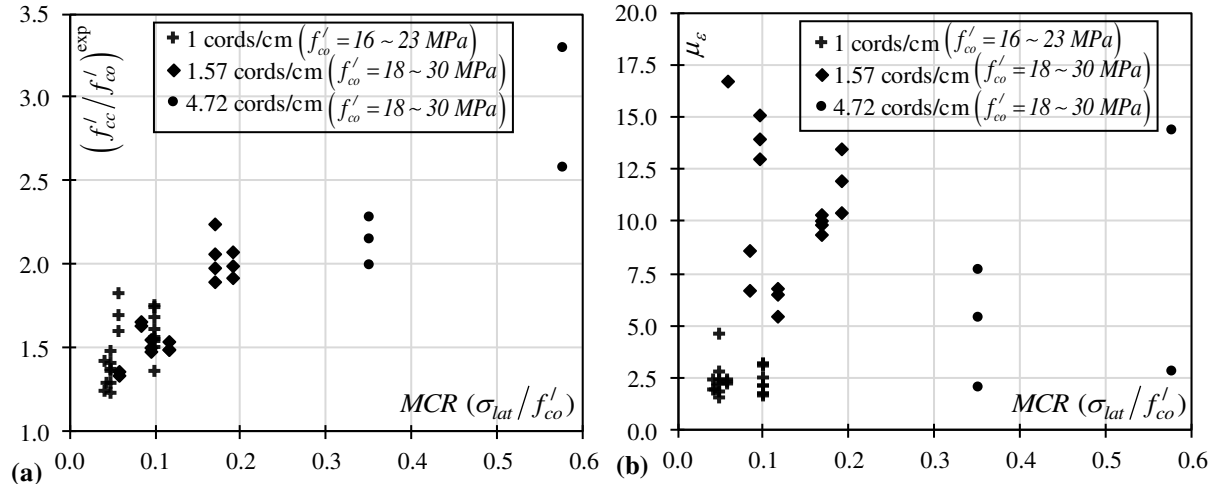

Figure 9: (a) Normalized compressive strength, f'_{cc}/f'_{co}, and (b) strain ductility, μ_ε, vs Modified Confinement Ratio (MCR) for SRG jacketed specimens tested in current study.

Strain ductility, μ_ε, was also estimated for assessing the confinement effect of the SRG-jacketed systems used in this study. Similar to the ASCE/SEI Standard 41-06 recommendations [36], the experimental axial stress-strain response curve was idealized by a bilinear curve as shown in Fig. 10. The yield stress was determined on the condition that the secant slope intersects the actual envelope curve at 60% of the nominal yield stress, while the area enclosed by the bilinear curve was equal to that enclosed by the original curve bounded by the peak strain corresponding to 20% drop from the peak stress. Similar to the previous case, only specimens that failed due to the rupture of the fabric and the mixed mode of failure were considered. The normalized compressive strength, f'_{cc}/f'_{co}, versus the strain ductility, μ_ε, values are plotted in Fig. 9(b). It is shown that in general the strain ductility was higher for MCR values ranging between 0.06 to 0.19 (with an upper limit of μ_ε=16.17). This range corresponds to SRG jacketing systems with 1.57 cords/cm fabric and f'_{co}=18~30 MPa. In addition, as a general trend, it can be observed that increasing the MCR was usually accompanied by a decrease in the strain ductility. In the light of the results in Fig. 9, it can be concluded that the SRG jackets with 1.57 cords/cm fabric and mortar M4 exhibited the best performance in terms of strength and strain ductility enhancement.

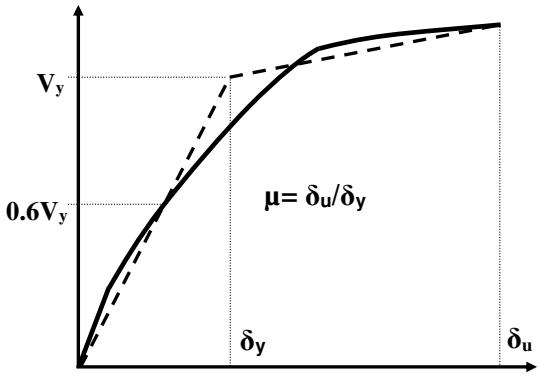

Figure 10: Bilinearization of the response curve – Definition of the ductility ratio.

5. CONCLUSIONS

An extensive experimental study was conducted to investigate the effectiveness of SRG jacketing system in improving the compressive strength and ultimate strain capacity of concrete columns. The SRG jacketing was applied to 52 cylindrical concrete specimens subjected to monotonic uniaxial compression load. The effects of different design parameters were studied, including the density, overlap length and number of layers of steel reinforced fabric, the type of binding mortar and the concrete compressive strength. Based on the results presented in this paper, the following conclusions can be drawn:

1. The use of 36 cm overlap length in one-layered 1 and 1.57 cords/cm density SRG jackets always led to rupture of the fabric, while in case of the higher density fabric (4.72 cords/cm) debonding was the dominant mode of failure. The two-layered 1 and 1.57 cords/cm SRG jackets failed due to rupture of the fabric for an overlap length of 24 cm. For the same overlap length, however, the two-layered 4.72 cords/cm SRG jackets exhibited a mixed mode of failure.
2. It was shown that one-layered SRG jackets could increase the strength capacity of the unconfined specimens by up to 40%, 64% and 122% for 1, 1.57 and 4.72 cords/cm steel fabrics, respectively. By adding the second layer of SRG jackets, these numbers were increased to 67%, 115% and 193%, respectively. Similarly, one-layered SRG jackets improved the ultimate strain of the unconfined specimens by up to 278% and 582% for 1 and 1.57 cords/cm fabrics (debonding failure occurred in the case of 4.72 cords/cm fabric). Using two-layered SRG jackets increased the ultimate strain of the unconfined specimens by up to 417%, 650% and 755% for 1, 1.57 and 4.72 cords/cm fabrics, respectively.
3. The comparisons made between the specimens with the same SRG jacketing showed that in general the effectiveness of SRG jackets increases as the unconfined concrete strength decreases. The type of mortar did not considerably influence the strength and deformation

capacity of the specimens when the failure mode was due to the rupture of steel fabric. However, the improvement in compressive strength and ultimate strain is slightly higher when a mortar with higher flexural strength is utilized.

ACKNOWLEDGEMENTS

The experimental program was conducted in the Laboratory of Strength of Materials and Structures, Civil Engineering Department, Aristotle University of Thessaloniki, with the help of Dr K. Katakalos and Mr M. Koukouftopoulos. Special thanks are attributed to Dr M. Stefanidou for designing the M2 and M3 mortars, A. Alexiou, E. Roupakia and N. Prompona for helping in the experimental program, and Interbeton, SIKA and Kerakoll for providing the materials. The project also received funding from the European Union's Horizon 2020 research and innovation programme under the Marie Skłodowska-Curie grant agreement No 700863. The authors would like to thank the European Union for their financial support.

REFERENCES

[1]. Thermou GE, and Pantazopoulou SJ. Fiber reinforced polymer retrofitting of substandard RC prismatic members. J Compos Constr 2009;13(6): 535-546.

[2]. Thermou GE, Pantazopoulou SJ, Elnashai AS. Global interventions for seismic upgrading of substandard RC buildings. J Struct Eng 2012; 138(3): 387-401.

[3]. Kaurtz S, Balaguru P. Comparison of inorganic and organic matrices for strengthening of RC beams with carbon sheets. J Struct Eng 2001; 127(1): 35-42.

[4]. Garon R, Balaguru PN, Toutanji H. Performance of inorganic polymer-fiber composites for strengthening and rehabilitation of concrete beams. London: FRPRCS-5 Conference, Burgoyne CJ, ed, Thomas Telford; 2001; 1: 53-62.

[5]. Toutanji H, Deng Y, Jia M. Fatigue performance of RC beams strengthened with cf sheets bonded by inorganic matrix. Singapore: FRPRCS-6 Conference, Tan KH, ed., World Scientific Publishing Co, 2003; 2: 875-884.

[6]. Wu HC, Teng J. Concrete confined with fiber reinforced cement based thin sheet composites. Singapore: FRPRCS-6 Conference, Tan KH, ed., World Scientific Publishing Co., 2003; 1: 591-600.

[7]. Triantafillou TC, Papanicolaou CG, Zissimopoulos P, Laourdekis T. Concrete confinement with textile-reinforced mortar jackets. ACI Struct J 2006; 103(1): 28-37.

[8]. Triantafillou TC, Papanicolaou CG. Shear strengthening of reinforced concrete members with textile reinforced mortar (TRM) jackets. Mater Struct 2006; 39(285): 93-103.

[9]. Bournas DA, Lontou PV, Papanicolaou CG, Triantafillou TC. Textile-reinforced mortar versus fiber-reinforced polymer confinement in reinforced concrete specimens. ACI Struct J 2007; 104(6): 740-748.

[10]. Menna C, Asprone D, Ferone C, Colangelo F, Balsamo A, Prota A, Cioffi R, Manfredi G. Use of geopolymers for composite external reinforcement of RC members. J Compos B Eng 2013; 45(1):1667–1676.

[11]. Vasconcelos E, Fernandes S, Barroso De Aguiar JL, Pacheco-Torgal F. Concrete retrofitting using metakaolin geopolymer mortars and CFRP. Constr Build Mater 2011; 25(8): 3213-3221.

[12]. Vasconcelos E, Fernandes S, De Aguiar B, Pacheco-Torgal F. Concrete retrofitting using CFRP and geopolymer mortars. Materials Science Forum 2013; 730-732: 427-432.

[13]. D'Ambrisi A, Feo L, Focacci F. Experimental analysis on bond between PBO-FRCM strengthening materials and concrete. J Compos B Eng 2013; 44(1): 524-532.

[14]. D'Ambrisi A, Feo L, Focacci F. Bond-slip relations for PBO-FRCM materials externally bonded to concrete. J Compos B Eng 2012; 43(8): 2938-2949.

[15]. Huang X, Birman V, Nanni A, Tunis G. Properties and potential for application of steel reinforced polymer and steel reinforced grout composites. J Compos B Eng 2005; 36(1): 73-82.

[16]. Thermou GE, Pantazopoulou SJ. Metallic fabric jackets: an innovative method for seismic retrofitting of substandard RC prismatic members. Fib Struct Concr J 2007; 8(1): 35-46.

[17]. Thermou GE, Katakalos K, and Manos G. Influence of the loading rate on the axial compressive behavior of concrete specimens confined with SRG jackets. Greece, Kos: ECCOMAS Thematic Conference COMPDYN 2013; Paper No. 1482.

[18]. Thermou GE, Katakalos K and Manos G. Concrete confinement with steel-reinforced grout jackets. Mater Struct 2015; 48(5): 1355-1376.

[19]. Thermou GE, Katakalos K, Manos G. Influence of the cross-section shape on the behaviour of SRG-confined prismatic concrete specimens. Mater Struct 2016; 49(3): 869-887.

[20]. Thermou GE, Katakalos K, Manos G. Experimental investigation of substandard RC columns confined with SRG jackets under compression. Compos Struct 2018, 184: 56-65.

[21]. Bencardino F, Condello A. Reliability and adaptability of the analytical models proposed for the FRP systems to the Steel Reinforced Polymer and Steel Reinforced Grout strengthening systems. J Compos B Eng 2015; 76: 249-259.

[22]. Bencardino F, Condello A. Eco-friendly external strengthening system for existing reinforced concrete beams. J Compos B Eng 2016; 93: 163-173.

[23]. De Santis S, Ceroni F, de Felice G, Fagone M, Ghiassi B, Kwiecień A, Lignola GP, Morganti M, Santandrea M, Valluzzi MR, Viskovic A. Round Robin Test on tensile and bond behaviour of Steel Reinforced Grout systems. J Compos B Eng 2017; 127: 100-120.

[24]. Bencardino F, Condello A, Ashour AF. Single-lap shear bond tests on Steel Reinforced Geopolymeric Matrix-concrete joints. J Compos B Eng 2017; 110(1): 62-71.

[25]. D'Antino T, Papanicolaou C. Mechanical characterization of textile reinforced inorganic-matrix composites. J Compos B Eng 2017; 127: 78-91.

[26]. BS EN 12636:1999. Products and systems for the protection and repair of concrete structures- Test methods- Determination of adhesion concrete to concrete. British Standards Institute (BSI), 1999.

[27]. Monti G., Nisticò N. Square and rectangular concrete columns confined by C-FRP: experimental and numerical investigation. Mech Compos Mater 2008; 44(2): 289-308.

[28]. Napoli A, Realfonzo R. Compressive behavior of concrete confined by SRP wraps. Constr Build Mater 2016; 127: 993-1008.

[29]. De Santis S, de Felice G, Napoli A, Realfonzo R. Strengthening of structures with Steel Reinforced Polymers: A state-of-the-art review. Compos B 2016; 104: 87-110.

[30]. Nisticò N, Monti G. R.C. square sections confined by FRP: analytical prediction of peak strength. Compos B 2013; 45(1): 127-137.

[31]. Nisticò N. R.C. Square Sections Confined by FRP: A numerical procedure for predicting stress strain relationship. Compos B 2014; 59: 238-247.

[32]. fib Bulletin 14. Externally bonded FRP reinforcement for RC structures. Report by Task group 9.3, fédération internationale du béton (fib), Lausanne, Switzerland 2001.

[33]. Mirmiran A, Shahawy M, Samaan M, El Echary H, Mastrapa JC, Pico O. Effect of column parameters on FRP-confined concrete. J Compos Construct 1998; 2(4): 175–185.

[34]. Spoelstra MR, Monti G FRP-confined concrete model. J Compos Constr 1999; 3(3): 143–150.

[35]. Teng JG, Jiang T, Lam L, Luo YZ. Refinement of a design-oriented stress-strain model for FRP-confined concrete. J Compos Construct 2009; 13(4): 269–278.

[36]. ASCE 41-06. Seismic rehabilitation of existing buildings. Edition: 1st. American Society of Civil Engineers; 2007.